REPORT DOCUMENTATION PAGE

Form Approved OMB NO. 0704-0188

The public reporting burden for this collection of information is estimated to average 1 hour per response, including the time for reviewing instructions, searching existing data sources, gathering and maintaining the data needed, and completing and reviewing the collection of information. Send comments regarding this burden estimate or any other aspect of this collection of information, including suggesstions for reducing this burden, to Washington Headquarters Services, Directorate for Information Operations and Reports, 1215 Jefferson Davis Highway, Suite 1204, Arlington VA, 22202-4302. Respondents should be aware that notwithstanding any other provision of law, no person shall be subject to any oenalty for failing to comply with a collection of information if it does not display a currently valid OMB control number.
PLEASE DO NOT RETURN YOUR FORM TO THE ABOVE ADDRESS.

1. REPORT DATE (DD-MM-YYYY) 29-07-2015	2. REPORT TYPE Final Report	3. DATES COVERED (From - To) 15-Apr-2012 - 14-Oct-2014

4. TITLE AND SUBTITLE	5a. CONTRACT NUMBER
Final Report: Ab initio design of noncentrosymmetric metals: crystal engineering in oxide heterostructures	W911NF-12-1-0133
	5b. GRANT NUMBER
	5c. PROGRAM ELEMENT NUMBER 611102

6. AUTHORS James Rondinelli	5d. PROJECT NUMBER
	5e. TASK NUMBER
	5f. WORK UNIT NUMBER

7. PERFORMING ORGANIZATION NAMES AND ADDRESSES	8. PERFORMING ORGANIZATION REPORT NUMBER
Drexel University Office of Research 3201 Arch Street, Suite 100 Philadelphia, PA 19104 -2875	

9. SPONSORING/MONITORING AGENCY NAME(S) AND ADDRESS (ES)	10. SPONSOR/MONITOR'S ACRONYM(S) ARO
U.S. Army Research Office P.O. Box 12211 Research Triangle Park, NC 27709-2211	11. SPONSOR/MONITOR'S REPORT NUMBER(S) 61940-PH-YIP.20

12. DISTRIBUTION AVAILIBILITY STATEMENT

Approved for Public Release; Distribution Unlimited

13. SUPPLEMENTARY NOTES
The views, opinions and/or findings contained in this report are those of the author(s) and should not contrued as an official Department of the Army position, policy or decision, unless so designated by other documentation.

14. ABSTRACT

The program used electronic structure based methods to design noncentrosymmetric metals (NCSM) in transitional metal oxides. The report describes the progress made towards understanding why any NCS metals should exist, how to find them, and the physical properties of these materials with potential applications. Main outcomes of the program include (a) establishing a weak electron-lattice coupling principle as a platform for explaining the stability of NCSM phases, (b) formulating a taxonomy and scheme to aid in the design of new NCSM, (c) designing/predicting new metallic transition metal oxides without inversion symmetry, and (d) efforts by

15. SUBJECT TERMS
Final Report on the Design of Noncentrosymmetric Metallic Oxides

16. SECURITY CLASSIFICATION OF:			17. LIMITATION OF ABSTRACT	15. NUMBER OF PAGES	19a. NAME OF RESPONSIBLE PERSON James Rondinelli
a. REPORT UU	b. ABSTRACT UU	c. THIS PAGE UU	UU		19b. TELEPHONE NUMBER 215-571-3671

Standard Form 298 (Rev 8/98)
Prescribed by ANSI Std. Z39.18

Report Title

Final Report: Ab initio design of noncentrosymmetric metals: crystal engineering in oxide heterostructures

ABSTRACT

The program used electronic structure based methods to design noncentrosymmetric metals (NCSM) in transitional metal oxides. The report describes the progress made towards understanding why any NCS metals should exist, how to find them, and the physical properties of these materials with potential applications. Main outcomes of the program include (a) establishing a weak electron-lattice coupling principle as a platform for explaining the stability of NCSM phases, (b) formulating a taxonomy and scheme to aid in the design of new NCSM, (c) designing/predicting new metallic transition metal oxides without inversion symmetry, and (d) efforts by experimental colleagues in realizing the NCSM predictions. Our main results include the identification of new layered ruthenates, molybdates, cuprates, and osmates that fulfill the formulated operational principle. The electronic, magnetic, and optical properties of these materials are reported. Where available the experimental studies of these systems through collaborative efforts are outlined.

Enter List of papers submitted or published that acknowledge ARO support from the start of the project to the date of this printing. List the papers, including journal references, in the following categories:

(a) Papers published in peer-reviewed journals (N/A for none)

Received Paper

06/24/2015 17.00 John W. Freeland, Jak Chakhalian, Andrew J. Millis, Christos Panagopoulos, James M. Rondinelli. Colloquium: Emergent properties in plane view: Strong correlations at oxide interfaces, Reviews of Modern Physics, (10 2014): 0. doi: 10.1103/RevModPhys.86.1189

06/24/2015 19.00 James M. Rondinelli, Emmanouil Kioupakis. Predicting and Designing Optical Properties of Inorganic Materials, Annual Review of Materials Research, (08 2014): 0. doi: 10.1146/annurev-matsci-070214-021150

06/24/2015 18.00 Mark D Scafetta, Adam M Cordi, James M Rondinelli, Steven J May. Band structure and optical transitions in LaFeO, Journal of Physics: Condensed Matter, (12 2014): 0. doi: 10.1088/0953-8984/26/50/505502

06/24/2015 16.00 Brittany B. Nelson-Cheeseman, Hua Zhou, Prasanna V. Balachandran, Gilberto Fabbris, Jason Hoffman, Daniel Haskel, James M. Rondinelli, Anand Bhattacharya. Polar Cation Ordering: A Route to Introducing >10% Bond Strain Into Layered Oxide Films, Advanced Functional Materials, (11 2014): 0. doi: 10.1002/adfm.201401077

08/19/2013 1.00 Nicole A. Benedek, James M. Rondinelli, Andrew T. Mulder, Craig J. Fennie. Turning ABO3 Antiferroelectrics into Ferroelectrics: Design Rules for Practical Rotation-Driven Ferroelectricity in Double Perovskites and A3B2O7 Ruddlesden-Popper Compounds, Advanced Functional Materials, (05 2013): 0. doi: 10.1002/adfm.201300210

08/19/2013 3.00 Mohammad A Islam, James M Rondinelli, Jonathan E Spanier. Normal mode determination of perovskite crystal structures with octahedral rotations: theory and applications, Journal of Physics: Condensed Matter, (05 2013): 175902. doi: 10.1088/0953-8984/25/17/175902

08/19/2013 2.00 Nina J. Lane, Michel W. Barsoum, James M. Rondinelli. Correlation effects and spin-orbit interactions in two-dimensional hexagonal 5d transition metal carbides, Ta, EPL (Europhysics Letters), (03 2013): 57004. doi: 10.1209/0295-5075/101/57004

08/29/2014 6.00 Nicole A. Benedek, James M. Rondinelli, Craig J. Fennie, Andrew T. Mulder. Turning ABO3 Antiferroelectrics into Ferroelectrics: Design Rules for Practical Rotation-Driven Ferroelectricity in Double Perovskites and A3B2O7 Ruddlesden-Popper Compounds, Advanced Functional Materials, (05 2013): 4810. doi: 10.1002/adfm.201300210

08/29/2014 7.00 James M. Rondinelli, Joshua Young. Atomic Scale Design of Polar Perovskite Oxides without Second-Order Jahn–Teller Ions, Chemistry of Materials, (11 2013): 4545. doi: 10.1021/cm402550q

08/29/2014 8.00 Prasanna V. Balachandran, Danilo Puggioni, James M. Rondinelli. Crystal-Chemistry Guidelines for Noncentrosymmetric A2BO4 Ruddlesden?Popper Oxides, Inorganic Chemistry, (01 2014): 336. doi: 10.1021/ic402283c

08/29/2014 9.00 Jin Suntivich, Wesley T. Hong, Yueh-Lin Lee, James M. Rondinelli, Wanli Yang, John B. Goodenough, Bogdan Dabrowski, John W. Freeland, Yang Shao-Horn. Estimating Hybridization of Transition Metal and Oxygen States in Perovskites from O K-edge X-ray Absorption Spectroscopy, The Journal of Physical Chemistry C, (01 2014): 1856. doi: 10.1021/jp410644j

08/29/2014 10.00 Danilo Puggioni, James M. Rondinelli. Designing a robustly metallic noncenstrosymmetric ruthenate oxide with large thermopower anisotropy,
Nature Communications, (03 2014): 3432. doi: 10.1038/ncomms4432

08/29/2014 11.00 E. J. Moon, P. V. Balachandran, B. J. Kirby, D. J. Keavney, R. J. Sichel-Tissot, C. M. Schlepütz, E. Karapetrova, X. M. Cheng, J. M. Rondinelli, S. J. May. Effect of Interfacial Octahedral Behavior in Ultrathin Manganite Films,
Nano Letters, (05 2014): 2509. doi: 10.1021/nl500235f

08/29/2014 14.00 Danilo Puggioni, James M Rondinelli. Linear optical and electronic properties of the polar metallic ruthenate (Sr,Ca)Ru2O6,
Journal of Physics: Condensed Matter, (07 2014): 265501. doi: 10.1088/0953-8984/26/26/265501

08/29/2014 15.00 Joshua Young, James M. Rondinelli. Improper ferroelectricity and piezoelectric responses in rhombohedral (A,A')B2O6 perovskite oxides,
Physical Review B, (05 2014): 174110. doi: 10.1103/PhysRevB.89.174110

TOTAL: **15**

Number of Papers published in peer-reviewed journals:

(b) Papers published in non-peer-reviewed journals (N/A for none)

Received   Paper

TOTAL:

Number of Papers published in non peer-reviewed journals:

(c) Presentations

Invited Papers by Rondinelli
- "Re-imagining Electronic Materials Discovery in Layered Oxides," Tel Aviv University, The First Northwestern University-Tel Aviv University Meeting on Semiconductors, Electronic Materials, Thin films and Photonic Materials, Ramat Aviv, Tel Aviv, Israel (February 23, 2015).

- "Versatile Abilities of Lattice Instabilities: New Design Strategies for Emergent Ferroics," AVS 61st International Symposium & Exhibition – Session on the Development of Multiferroic Materials, Baltimore, Maryland, USA (November 14, 2014).

- "Versatile Abilities of Lattice Instabilities: New Design Strategies for Emergent Ferroics," Materials Science & Technology 2014– Symposium on Multifunctional Oxides, Pittsburgh, Pennsylvania, USA (October 14, 2014).

- "Electrostatic Chemical Strain: Orbital Engineering in Correlated Oxides," 21st International Workshop on Oxide Electronics, at Bolton Landing, New York, USA (September 29, 2014).

- "Designing new phases in oxides by using the versatile abilities of lattice instabilities," Advances in oxide materials: Preparation, properties, performance, at University of California, Santa Barbara California, USA (August 28, 2014).

Contributed Paper by Young
- "First Principles Design of Electronic Function in Non-Centrosymmetric Metal Oxides," Summer Workshop on Advances in Oxide Materials - Santa Barbara, California, USA (August 29, 2014).

- "First Principles Design of Electronic Function in Non-Centrosymmetric Metal Oxides," International Workshop on Oxide Electronics - Bolton Landing, New York, USA (September 30, 2014).

- "Ferri-to-Ferroelectric Phase Transitions in Perovskite Oxides," International Conference of Young Researchers on Advanced Materials - Haikou, China (October 25, 2014).

- "Emergent Ferroelectricity in Cation Ordered Perovskite Oxides by Design," Asian Meeting on Ferroelectrics and Electroceramics - Shanghai, China (October 27, 2014).

Number of Presentations: 9.00

Non Peer-Reviewed Conference Proceeding publications (other than abstracts):

Received   Paper

TOTAL:

Number of Non Peer-Reviewed Conference Proceeding publications (other than abstracts):

Peer-Reviewed Conference Proceeding publications (other than abstracts):

Received   Paper

TOTAL:

Number of Peer-Reviewed Conference Proceeding publications (other than abstracts):

(d) Manuscripts

Received   Paper

08/22/2013 5.00 Danilo Puggioni, James Rondinelli, Prasanna Balachandran. Crystal-chemistry guidelines for noncentrosymmetric A2BO4 Ruddlesden-Popper Oxides,
Preprint (08 2013)

08/25/2013 4.00 Danilo Puggioni, James M Rondinelli. Designing a robustly metallic noncentroysmmetric ruthenate oxide with large thermopower anisotropy,
Preprint (08 2013)

TOTAL: **2**

Number of Manuscripts:

Books

Received   Book

TOTAL:

<u>Received</u>   <u>Book Chapter</u>

TOTAL:

Patents Submitted

Patents Awarded

Awards

2014 American Ceramic Society's Ross Coffin Purdy Prize
2014 Emerging Scientist in ACS Select Virtual Issue on Solid-State Chemistry

Graduate Students

NAME	PERCENT_SUPPORTED	Discipline
Joshua Young	0.50	
FTE Equivalent:	**0.50**	
Total Number:	**1**	

Names of Post Doctorates

NAME	PERCENT_SUPPORTED
Danilo Puggioni	1.00
Mingqiang Gu	0.20
FTE Equivalent:	**1.20**
Total Number:	**2**

Names of Faculty Supported

NAME	PERCENT_SUPPORTED	National Academy Member
James Rondinelli	0.08	No
FTE Equivalent:	**0.08**	
Total Number:	**1**	

Names of Under Graduate students supported

NAME	PERCENT_SUPPORTED
FTE Equivalent:	
Total Number:	

Names of Personnel receiving masters degrees

NAME
Adam Cordi
Total Number: **1**

Names of personnel receiving PHDs

NAME

Total Number:

Names of other research staff

NAME   PERCENT_SUPPORTED

FTE Equivalent:
Total Number:

Sub Contractors (DD882)

Inventions (DD882)

Scientific Progress

Technology Transfer

FINAL REPORT

ARO W911NF-12-1-0133

❉

∼

James M Rondinelli

Department of Materials Science & Engineering, Northwestern University, Evanston, Illinois 60208, USA

I. Program Summary

The program utilized electronic structure based methods to design noncentrosymmetric metals (NCSM) in transitional metal oxides (Figure 1). The report describes the progress made towards understanding why any NCS metals should exist, how to find them, and the physical properties of these materials with potential applications.

Main outcomes of the program include (a) establishing a weak electron-lattice coupling principle as a platform for explaining the stability of NCSM phases, (b) formulating a taxonomy and scheme to aid in the design of new NCSM, (c) designing/predicting new metallic transition metal oxides without inversion symmetry, and (d) efforts by experimental colleagues in realizing the NCSM predictions.

The key results include the identification of new layered ruthenates, cuprates, osmates, and molybdates that fulfill the formulated operational principle. The culmination of this effort has also spawned numerous acentrix oxides and ferroic discoveries from mechanisms that emerge in layered oxide compounds otherwise not possible in simpler structures and chemistries.
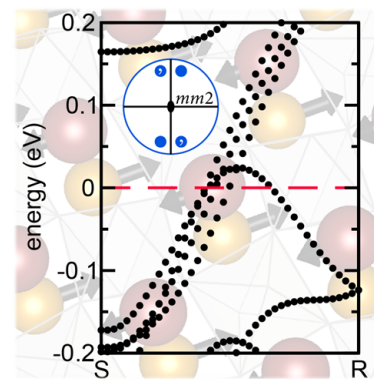

Figure 1: Metals with noncentrosymmetric crystal structures are rare, but this class of compounds with finite band occupancy and broken inversion symmetry (inset) may have desirable physical properties for device applications. This program delivered a design framework for predicting new noncentrosymmetric conductors and proposed new technology arenas where they may be utilized.

II. Scientific Discoveries & Accomplishments

A. New Oxides without Inversion Symmetry.
Representation theory analyses performed during this program examined how changes in the direction of cation ordering *and* octahedral rotations can lead to the loss of inversion symmetry in A/A' 1/1 superlattices: layered (001)-type, columnar (110)-type, and rock-salt

Figure 2: The three types of A/A' cation ordering investigated: (a) layered, (b) columnar, and (c) rock salt arrangements. Oxygen atoms are omitted for clarity.

(111)-type ordering (Figure 2). In this case, the superposition of the cation ordering and rotations lead to 31 unique space groups and 11 unique crystal classes. Six of these crystal classes are noncentrosymmetric. The important result is that there are no combinations of octahedral rotations and columnar ordering that produce noncentrosymmetric (NCS) crystals, sans any other distortions. We identified that the most promising compositions to search for acentricity in A-site layered or rock-salt ordered 1/1 superlattices; we reported these results in an article published in *Chemistry of Materials*.[1] This work was also extended to include B/B', and mixed A/A', B/B' 1/1 superlattices (Figure 3). *This structural 'heat map' establishes a design tool that makes it possible to select chemistries and polymorphs in perovskite oxides that are conducive to NCSM behavior.*
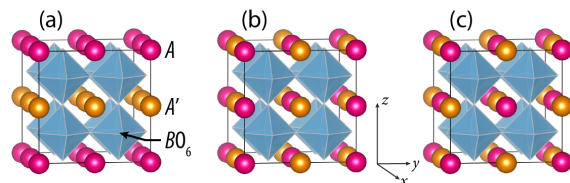
Our results reveal that the ordered arrangement of cations plays a critical role in determining the allowed rotation patterns that can lift inversion symmetry. The main conclusion is that *rotations of oxygen octahedra*
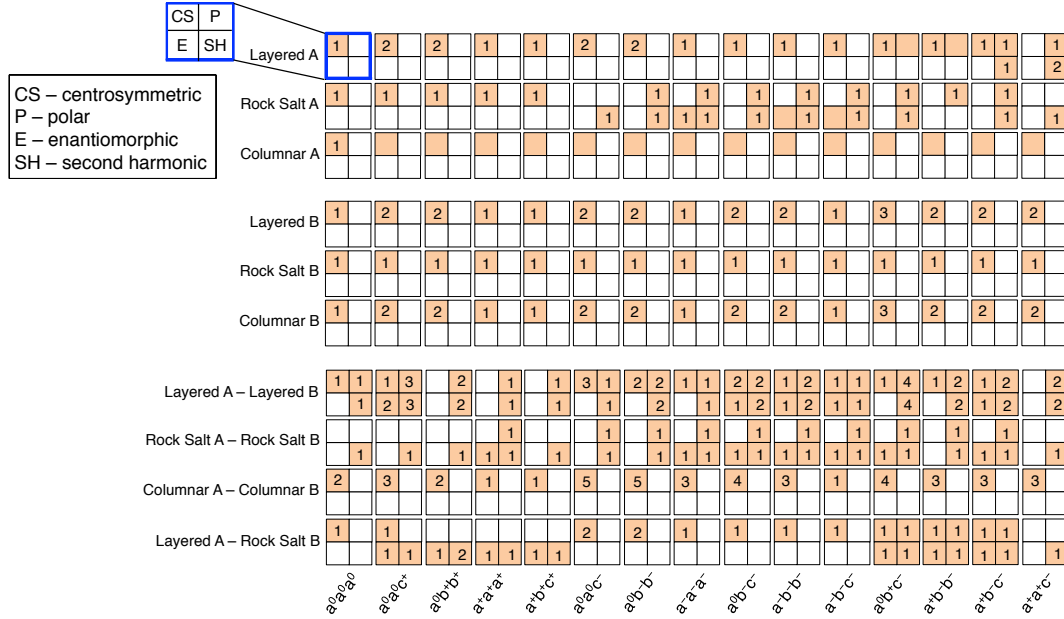

Figure 3: The type of space group symmetry produced by combining each of the layered ([001]), rock salt ([111]), and columnar ([110]) type A- and B-site cation ordering patterns with the 15 Glazer rotational patterns of the BO6 octahedra. 540 distinct structures are represented, produced by also considering [100] and [010] layered ordering, and [101] and [011] columnar ordering. Each separated block depicts one ordering-rotation combination; these are further subdivided into whether a centrosymmetric, polar, enantiomorphic (chiral), or SHG-active space group is exhibited (indicated by a filled square) by the given combination. The number of distinct space groups produced is given by the number in each of the filled squares. Note that because many non-centrosymmetric space groups fall into more than one category (for example, point group 2 is both chiral and polar), the numbers do not sum to the total number of structures.

can induce ferroelectric polarizations if the cations are arranged in a **layered or rock salted order**. Using this chemistry-agnostic understanding, we then designed several new polar oxides. Our main discoveries include:

◇ **New Chiral Perovskites.** We studied rhombohedral instead of orthorhombic perovskites in superlattices of rare-earth aluminates. We found that although most of the compounds are polar and exhibit a small spontaneous polarization of 2 μC/cm^2, these compounds undergo a *transition to a chiral phase accompanied by a dramatic increase in the piezoelectric response* that persists to high temperature (Figure 4), which could inspire new high temperature, low-fatigue piezoelectric devices.[2] *The main finding is that while only (La,Pr)Al$_2$O$_6$ and (Ce,Pr)Al$_2$O$_6$ are polar, all were found to undergo a transition to an R32 chiral phase at higher temperatures.* By computing the total polarization, we found that chiral (La,Nd)Al$_2$O$_6$ has zero polarization while the polar phases have values of ~2μC/cm^2. This rare example of chiral perovskites was reported in *Physical Review B*.[2]

◇ **New Ferroic Transition—Ferrielectricity.** We identify a first-order, isosymmetric transition between a ferrielectric (FiE) and ferroelectric (FE) state in A-site ordered LaScO$_3$/BiScO$_3$ and LaInO$_3$/BiInO$_3$ superlattices.[3] *Such a previously unreported ferroic transition is driven by the easy switching of cation displacements without changing the overall polarization direction or crystallographic symmetry.* Epitaxial strains less than 2% were predicted to be sufficient to traverse the phase boundary, across which we captured a ~5X increase in electric polarization. Unlike conventional Pb-based perovskite ceramics with a morphotropic phase boundary (MPB) that show polarization rotation, we predicted an electromechanical response up to 102 pC/N in the vicinity of FiE-FE phase boundary due to polarization *switching* without the change in symmetry. *The significance of this result is that the transition is an alternative ferroic transition to obtain sizeable piezoelectric responses, with the additional advantage of occurring at integral stoichiometry in an ordered superlattice, without introducing compositional complexity, toxicity, or*

a change in symmetry—features absent in conventional Pb-based piezoelectrics. This work was published in *Advanced Materials Interfaces.*[3]

◇ **Magnetic Oxides with Enhanced Polarizations.** Recent experimental and theoretical work has shown that the double perovskite $NaLaMnWO_6$ exhibits antiferromagnetic ordering owing to the Mn d states, and computational studies further predict it to exhibit a spontaneous electric polarization due to an improper mechanism for ferroelectricity [King *et al., Phys. Rev. B*, 2009, **79**, 224428; Fukushima *et al., Phys. Chem. Chem. Phys.*, 2011, **13**, 12186], which make it a candidate multiferroic material. Using first-principles density functional calculations, we investigated nine isostructural and isovalent $AA'MnWO_6$ double perovskites (A=Na, K, and Rb; A'=La, Nd, and Y) and *formulated crystal-chemistry guidelines describing how to enhance the magnitude of the electric polarization through chemical substitution of the A-site while retaining long-range magnetic order.* The simultaneous presence of anti-ferromagnetic ordering of the Mn atoms and spontaneous electric polarization makes these compounds multiferroic, a highly desired type of material for applications such as four-state memory devices. By substituting a variety of alkali metal (Na, K, Rb) and rare earth (La, Nd, Y) elements on the *A*- and *A'*-sites, *we showed that the magnitude of the ferroelectric polarization can be increased by up to 150% without destroying the magnetic properties.*[4] This work was published in *Dalton Transactions.*[4]

The insulating acentric oxides and ferroic mechanisms described above were direct outcomes of our efforts in this program focused on the design and understanding of noncentrosymmetric metals (NCSM), which are described next.

B. Noncentrosymmetric Metals.

B.1. New Classification Scheme for Materials Discovery.

We **established a framework to design/discover NCSM oxides**, which originates from Anderson's work[5] on "ferroelectric metals," where he writes that, "while free electrons screen out the electric field [in materials] completely, they do not interact very strongly with the transverse optical phonons and the Lorentz local fields [that] lead to ferroelectricity, since umklapp processes are forbidden as $k \to 0$." We recasted this observation into an *operational design principle* that states:

Figure 4: Predicted piezoelectric coefficients for $La_{1/2}Pr_{1/2}AlO_3$.

> *The existence of any NCSM relies on weak coupling between the electrons at the Fermi level, and the (soft) infrared-active phonons responsible for removing inversion symmetry.*

An essential, implicit, materials constraint is that the low-energy electronic structure derives from an electron count giving partial band occupation, which may be obtained by judicious selection of the cation chemistries.

After surveying families of known NCSMs, we identified three routes by which the weak-coupling operation principle may be validated in a solid-state system (Table 1), and reported our findings in *Nature Communications.*[6] *The summary of our comprehensive survey will be reported later in 2015/2016 in the form of an invited article to J. Phys.: Condens. Matter.* The classification scheme entails specify the symmetry behavior of the lattice phonons that would characterize the inversion symmetry loss across a centrosymmetric to NCS structural transition (Table 1). Because the first approach is 'trivial', we have rather focused our efforts on exploring NCSM realized by Mechanism 2 and 3 in the layered cuprates ($LnSr_2Cu_2GaO_7$, Mechanism 2) and ruthenate, osmate, and molybdate superlattices (Mechanism 3).

B.2. Designed Polar Metals—Ruthenates.

Using our operational principle, we designed ultrashort period $SrRuO_3/CaRuO_3$ superlattices. Our main results reported in *Nature Communications*[6] include:
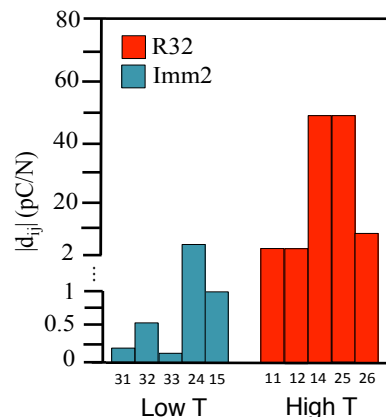
Table 1: Routes to lift inversion symmetry in metallic compounds. The scheme is formulated by classifying the symmetry requirements of the lattice mode instabilities of a centrosymmetric (reference) phase which would drive a thermodynamic transition to a noncentrosymmetric crystal structure. Although compositional ordering may be an obvious route to lift inversion symmetry, we recognize that experimentally in practice it may be challenging to achieve it, especially in oxide materials owing to bond-coordination requirements; therefore, although the route is simple, it is by no means straightforward. Note that all materials are expected to show some interesting physical properties enabled by an acentric crystal structure with itinerant electrons, independent of the mechanism leading to the mutual coexistence of the prerequisite atomic and electronic structure.

	Inversion-lifting Mechanism	Phonon Requirements	Description
(1)	Compositional Order ($\star$)	None	Achieved by decorating one or more interleaved lattices with multiple cations, e.g., as realized in half-Heusler alloys or tri-color, $\cdot/ABC/ABC/\cdot$, superlattices.
(2)	Packing of Acentric Polyhedra	1, $k = 0$ or $k \neq 0$ mode	Realized by the alignment of acentric metal-oxygen polyhedral units arising from either out-of-center metal distortions or because they intrinsically lack inversion (MO_4 tetrahedron), and contribute few (if any) states to or near the Fermi level.
(3)	Geometric-induced Displacements	≥ 2, $k \neq 0$ coupled modes	Obtained by anharmonic coupling of two or more centric lattice modes, which cooperatively remove inversion and produce cation displacements that do not gap the electronic structure. Accessible in some, effectively, two-dimensional compounds, e.g., naturally layered structures or 3D systems with bi-color ordering.

1. *The ground state structure is polar, space group $Pmc2_1$* (Figure 5). The inversion symmetry is due to centric RuO_6 octahedral rotations that induce polar Sr, Ca, and remarkably Ru displacements.

2. *The electronic structure is robustly metallic* in the polar ground state. Our calculations show that spin-orbit interactions, which play a significant role in determining the orbital structure in some transition-metal oxides,[7,8] weakly modified the Ru $4d$-band occupation at the Fermi level.

3. *The thermopower coefficients are highly anisotropic.* The anisotropy,[9] which we quantify by computing the contributions along the principal axes and then taking the sum $\Delta \mathcal{S}_\perp = \mathcal{S}_c - \frac{1}{2}(\mathcal{S}_a + \mathcal{S}_b)$, is approximately 6.3μV/K at 300 K derived from its polar structure. It exceeds that of $YBa_2Cu_3O_{7-\delta}$ ($\sim 7 - 10\mu$V/K).[10]

Our study on the $SrRuO_3/CaRuO_3$ 1/1 superlattice provides, to the best of my knowledge, the **first examination and theoretical calculation of the thermoelectric properties of a NCSM**. The **implications of this behavior** include the potential for *highly anisotropic thermoelectric devices*. For example, the peculiar thermopower anisotropy in the $SrRuO_3/CaRuO_3$ 1/1 superlattice dictates that the electric field resulting from an applied heat flux to the material will be non-collinear. This property is a fundamental feature for any anisotropic thermoelectric devices.[9] It enables the heat flux to be measured in a geometry perpendicular to

Figure 5: Crystal structure of the layered $(Sr,Ca)Ru_2O_6$ perovskite with RuO_6 octahedra exhibiting the $a^+b^-b^-$ octahedral tilt pattern (a). The out-of-center Ru^{4+} distortions (bond lengths in Å) produce local dipoles which cooperatively order along the c-direction (b), removing the mirror plane perpendicular to the A-site cation order. The local coordination environment for (c) Sr (tetra-capped trigonal prism) and (d) Ca (bi-capped trigonal prism) reveal that large A-site distortions from the ideal 12-fold coordination occur in opposite directions (arrows), along the polar c-axis.

the induced electrical current, specifically at locations where the temperatures are equal (Figure 6). Given the metallic conductivity of the ruthenate superlattice and that the relaxation time is small in comparison with that of semiconductors or insulators already finding use in thermoelectric devices, this polar-NCSM would enable sensing on sub-nanosecond timescales (comparable to YBCO[11]). *New applications of these oxide materials could be found in ultrafast-thermoelectric devices,*[9,11] *where stability under extreme conditions,*
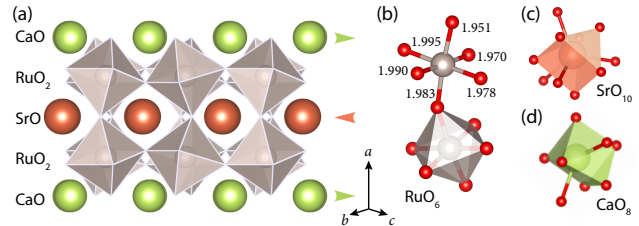
speed, and the ability to measure heat fluxes of high density are key requirements, e.g., thermal (heat) radiation detectors. Moreover, because of the compatibility of perovskite oxides with Si-based CMOS technologies,[12] we anticipate these designed NCS metals will more readily find integration and device development than previously identified materials with large anisotropic thermoelectric responses.

Furthermore, we investigated the linear optical properties of this superlattice using density functional theory. The results are published in *J. Phys. Condens. Matter.* **26**, 265501 (2014). In this effort, we found that the *polar* ferromagnetic metallic ruthenate exhibits optical anisotropy along the principal directions of the optical indicatrix owing to the absence of inversion symmetry in the crystal structure.[13] We then used the generalized Drude model[14–16] and deduced an enhancement of the effective mass, $m^* \sim 4.9 m_e$. Upon removal of the polar distortions, we determined there was a decrease in the effective mass to $m^* \sim 4.4 m_e$.

$$E_1 = \mathcal{S}_{12} \frac{\partial T}{\partial x_2}$$

Figure 6: Thermoelectric device based on an anisotropic thermal conductor. The temperature gradient along the x_2 direction results in an electric field along the x_1 direction, which can generate a current density. Note that along the x_1 direction there is no temperature gradient, i.e., $\partial T/\partial x_1 = 0$, and thus $T_A = T_B$.

Our **main discovery** is uncovering a dependence of the effective mass on the amplitude of the polar distortion. *This suggests that control over the degree of inversion symmetry breaking via the polar displacements could be used and an effective 'handle' over the strength of the electronic correlations in the ruthenate superlattice, and perhaps, in polar metals generally.* We conjecture that epitaxial strain, which has been successfully used to induce (or enhance) polar distortions in conventional dielectrics (ferroelectrics),[17–19] could also be applied to thin films of $SrRuO_3/CaRuO_3$ to modulate the amplitude of the polar Sr and Ca displacements; thereby, tuning the electron-electron interactions which would lead to control over the effective carrier masses.

Lastly, in this effort we have and continue to work with Prof. Chang-Beom Eom's Group to **experimentally realize the 3/3 period ruthenate superlattices** (Figure 7), which is more amenable to oxide thin film growth. We have performed DFT calculations to predict the ground state structure, the electronic, and magnetic properties of this superlattice, and summarize our main results here: we imposed as a constraint $b = c = 3.867$ Å, simulating the situation of thin-film growth of the cuprate on $NdGaO_3$. The ground state structure has space group $Pmc2_1$, similar to the 1/1 superlattice, and exhibits the $a^+b^-b^-$ octahedral tilt pattern. The density of states is consistent with that reported in Ref. 20 where the valence band is com-

Figure 7: Epitaxial growth of a (Sr,Ca)RuO₃ film and a [(SrRuO₃)₃/(CaRuO₃)₃]₁₀ superlattice on orthorhombic NdGaO₃ (001) substrates synthesized in the Eom's Group (University of Wisconsin, Madison). AFM images of a (Sr,Ca)RuO₃ film (a) and a [(SrRuO₃)₃/(CaRuO₃)₃]₁₀ (b) superlattice on NdGaO₃ (001) substrates. The insets represent the corresponding RHEED images of the CaRuO₃ and SrRuO₃ films (c), θ-2θ scans of a (Sr,Ca)RuO₃ film and a [(SrRuO₃)₃/(CaRuO₃)₃]₁₀ superlattice on NdGaO₃ (001) substrates.

posed largely of O $2p$ states hybridized with Ru $4d$ states, with the oxygen states predominately found in regions below the Fermi energy. The Ru atoms are magnetic with a moment of $0.154 \mu_B$ on Ru(1), $0.400 \mu_B$ on Ru(2), and $0.015 \mu_B$. These superlattices are now being studied using second-harmonic generation by the Gopalan group at PennState to confirm our theoretical predictions. Results from this work is planned for publication in 2015 or 2016.
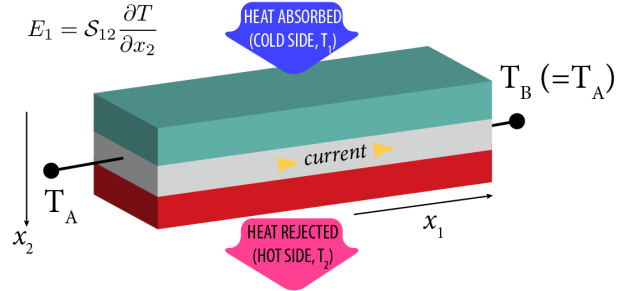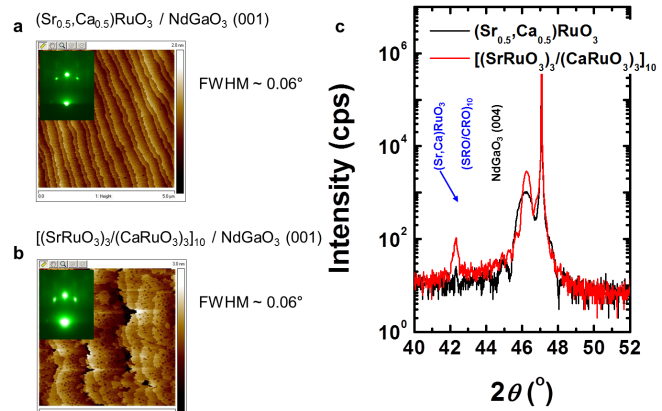
B.3. Understanding Conducting Copper Oxides without Inversion Symmetry.

We studied the lattice dynamics and electronic properties of the layered copper oxide superconductor LaSr$_2$Cu$_2$GaO$_7$ (LSCGO)[21,22] as a model system to explain the existence of NCSMs. Our main conclusion from these investigations is that the **symmetry breaking in LSCGO originates from the chemistry of** $3d^{10}$ **Ga**, which prefers to form tetrahedral coordinations. The incompatibility between displacements that derive from the zone-center phonons and the metallic behavior is circumvented in LSCGO by the fact that these distortions are largely decoupled from the electronic structure at the Fermi level (Figure 8)—they occur at much lower energy and hence fulfill our weak-electron lattice coupling principle. We showed that the distortion of the GaO4 polyhedra unit leads the loss of inversion symmetry through Mechanism 2.

Owing to the near degeneracy of the polar and non-polar LSCGO low-symmetry structures, we performed a series of calculations to understand the origin for the degeneracy as means to understand how to favor the polar phase over the non-polar structure. Figure 9 depicts the *Ima*2 and *Pnma* structures. The main structure difference between the two phases is the alignment of the tetrahedral GaO$_4$ units. In the polar *Ima*2 structure, the base-to-vertex direction of each tetrahedra is aligned along the same (c) direction [Figure 9, left]. In contrast, the non-polar *Pnma* structure possesses GaO$_4$ that are anti-aligned. The different layers point either along the +c or -c-direction.

Remarkably, the electronic structure also does not depend on the alignment of the GaO$_4$ units [Figure 9, right], suggesting to us that the LSCGO electronic

Figure 8: Electronic properties of LaSr$_2$Cu$_2$GaO$_7$ for the centric *Imma* (orange) and acentric *Ima*2 structure. Comparison between the total DOS (a), CuO$_2$ layers (b), Ga d-states (c), Ga s- and p-states (d).

structure is more accurately described by two "disconnected" sub-blocks. Figure 9 depicts the two sub-blocks (outlined in a broken line). Each block contains one plane of GaO$_4$ tetrahedra. We proposed that because the inter-block distance d is large under the equilibrium constraints (d = 3.57 Å), the electronic structure and phase stability is essential independent of the GaO$_4$ orientation (aligned or anti-aligned). We tested this hypothesis by keeping the atomic positions of the structural blocks fixed and reduced the inter-block distance. For each fixed d-value, we then computed the density-of-states. We find that the blocks become
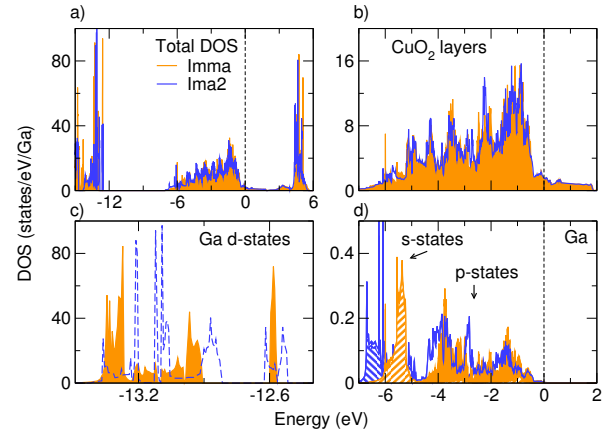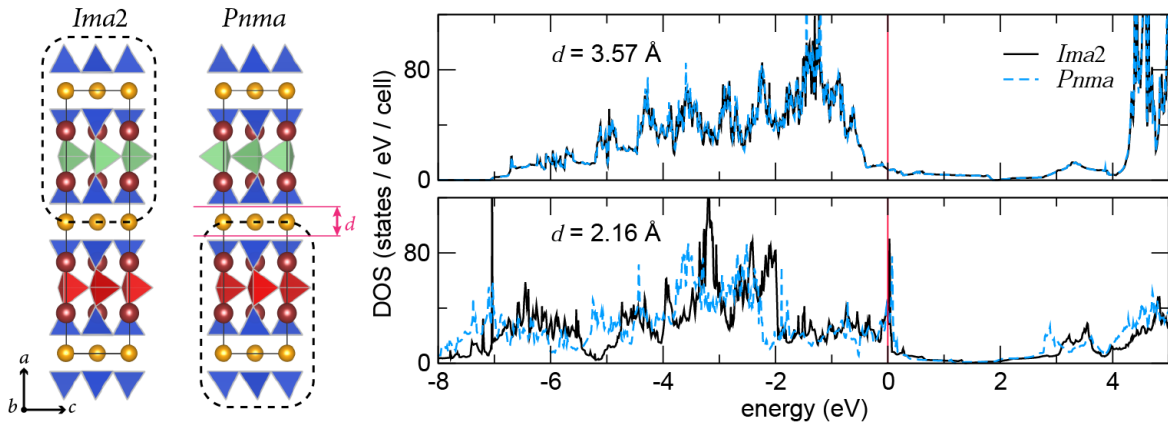

Figure 9: Crystal structure for the polar *Ima*2 and non-polar (*Pnma*) LSCGO phases (left). The main difference is the alignment of the GaO$_4$ tetrahedral units (red or green) along the crystallographic c-axis. The molecular sub-block units are outlined. Effect of inter-block spacing d on the electronic structure degeneracy between the two phases (right). Bringing the molecular blocks closer by reducing d leads to interactions that split the electronic equivalency of the two phases.

"coupled" when d is approximately 2.16 Å as seen by the different electronic structure between the $Ima2$ and $Pnma$ phases (Figure 9). Based on these experiments, we arrived at our main result: **The polar cuprate phase can be favored by reducing the inter-block spacing.** Our subsequent efforts in this project focused on identifying feasible routes to control that space and thus the phase stability.

First, we examined how *chemical pressure* can be used to tune the stability by using divalent cations of different sizes. Here we considered Sr→Ca substitution and A-cation mixing, to give the following compounds: $LaSr_2Cu_2GaO_7 \rightarrow LaCa_2Cu_2GaO_7$. Without A-cation mixing, as shown in Figure 10a, we found a strong competition between the two phases with ~ 3 meV favoring the NCSM. However, differently from LSCGO, this configuration is energetically disfavoured (~680 meV) with respect to the situation with A-cation mixing (Figure 10b). **Importantly, A-cation mixing stabilizes the $Ima2$ phase of $LaCa_2Cu_2GaO_7$ over the $Pnma$ one by ~25 meV.** The difference in stability between $LaSr_2Cu_2GaO_7$ and $LaCa_2Cu_2GaO_7$ can be explained considering the size of the cations involved in the substitution. Ca^{2+} is smaller than Sr^{2+} and prefers A-sites in layered cuprates such as the 8-coordinate site between cuprate planes, as in $HgBa_2CaCu_2O_{6+\delta}$.[23] The chemical substitution reduces the interlayer space and *demonstrates* that chemical pressure is a promising way to achieve a polar conducting cuprate.

Figure 10: Energy difference between the $Ima2$ and $Pnma$ structure for $LaCa_2Cu_2GaO_7$ without (a) and with (b) A-cation mixing.

Next, based on understanding the role of the interlayer GaO_4 interactions (Figure 9), we identified another convenient approach to reduce the real-space distance between sub-blocks. *Here we leveraged the out-of-plane lattice response of a thin film under tensile epitaxial strain to tune the phase stability.* Six different substrates were surveyed in the range bounded by $LaAlO_3$ (3.821 Å) and $PrScO_3$ (4.013 Å). Figure 11 shows the results of our DFT calculations on the energetic stability of the polar ($Ima2$) phase relative to the centrosymmetric ($Pnma$) structure for thin films of $LnSr_2Cu_2GaO_7$ (Ln=La and Y). Note that in the compound $Y_{1-x}Ca_xSr_2GaCu_2O_{7\pm\delta}$ superconductivity was observed[24] for the range of Ca-content $x \geq 0.4$. We therefore also computed the stability of ordered $Y_{1/2}Ca_{1/2}Sr_2GaCu_2O_7$ compound. We find that epitaxial strain lifts the energetic degeneracy between the phases. Consistent with our previous discussion, **increasing tensile strain provides additional stability for the polar structure through controlled variation in the interlayer d spacing**. We therefore predict that these layered Ga-containing cuprates when grown under tensile strain should be polar metals.

Figure 11: Effect of epitaxial strain on the energetic stability of the polar $Ima2$ phase in $LnSr_2Cu_2GaO_7$. The polar structure is more stable (negative) with increasing epitaxial strain and for smaller lanthanide (Ln=Y) cations. Potential substrate materials are indicated. The behavior of d_{Cu} is consistent with our model for the GaO_4 interactions.

Over the program we actively engaged and continue to engage two experimental groups to demonstrate the phase stability of the polar cuprate in bulk and thin film form. First, we collaborated with *Prof. Ken Poeppelmeier* in the Chemistry Department at Northwestern University. His group synthesized ceramic targets for pulsed-laser deposition (PLD) growth of $LaSr_2Cu_2GaO_7$ and $Y_{1-x}Ca_xSr_2Cu_2GaO_7$ with $x = 0.0, 0.2, 0.3, 0.4, 0.5$. For $0 < x < 0.3$ the ceramics can be made phase pure with small particulate size. However, for $x \geq 0.4$ it is much more difficult to incorporate Ca into the lattice (Figure 12).
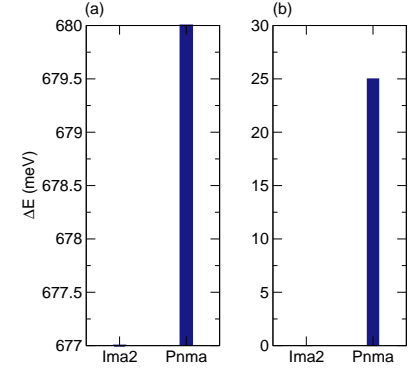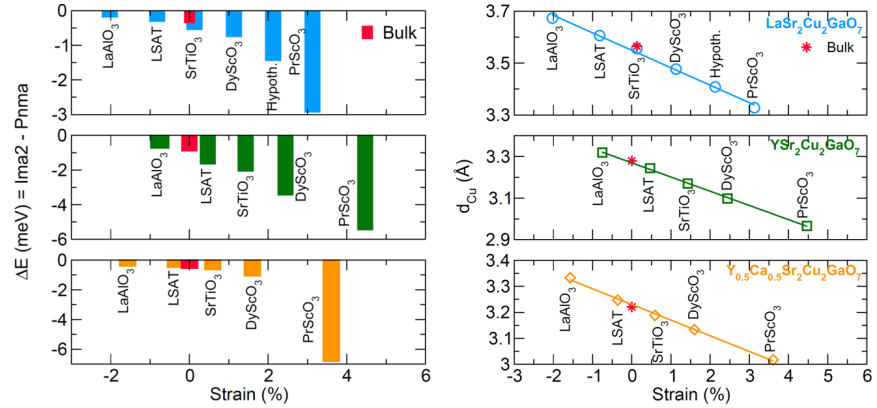
Using the prediction of large tensile strain as a route to stablize the polar cuprate phases, the Poeppelmeier group also grew single crystals of $PrScO_3$ as a substrate material, for which there are no commercial suppliers, for the PLD growth by *Prof. Yuri Suzuki's* group in the Applied Physics Department at Stanford University. The scandate single crystals

Figure 12: Sintered ceramic and $PrScO_3$ single crystals by floating-zone method and corresponding scandate Laue diffraction pattern.

were grown in an optical float zone furnace from which substrates were cut and Laue diffraction confirms the zone axes of the single crystals. At present, the Suzuki group is determining the optimal pulse-laser deposition (PLD) growth conditions on LAO, STO, and LSAT using the ceramic targets prepared by the Northwestern group. We are hopeful that thin films with the correct stoichiometry will be realized.
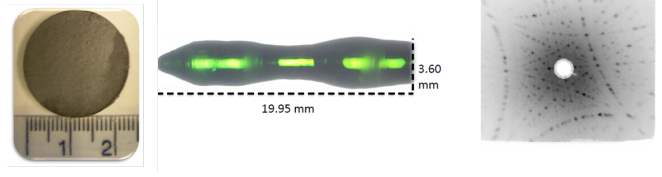
B.4. Polar Metals as a Platform for Multiferroic Discovery.

The main objective of this effort was to design a Mott-induced multiferroic by taking a non-magnetic *polar metal* close to a Mott transition and inducing a magnetic insulating state through heterostructuring. The motivation was to realize a new type of magnetoelectric material, *i.e.*, where their is strong coupling between the primary electric and magnetic polarizations owing to the coexistence of ferroelectricity and ferromagnetism, from a NCSM. Such materials are highly sought for in low-power multi-state ferroelectric random access memories (FE-RAM).[25–30]

We examined the layered ordered $(LiOsO_3)_1/(LiNbO_3)_1$ superlattice formed by interleaving $LiNbO_3$ and $LiOsO_3$, which both have polar crystal structures ($R3c$).[31,32] The former is an insulator with a band gap of 3.25 eV (Figure 13a) whereas $LiOsO_3$ is metallic with the Fermi level dominated by the Os 5d-states (Figure 13b). First, we examined the electronic properties of the newly discovered "ferroelectric metal" $LiOsO_3$ combining density-functional and dynamical mean-field theories. We showed that the material is close to a Mott transition. **We identified for the first time that the Hund's coupling in $LiOsO_3$ make it an ideal candidate for realizing a Mott MF due to the multi-orbital t_{2g} physics.**

Next, we describe the design of a new multiferroic by control of the electronic structure through atomic scale engineering of a Mott metal-insulator transition (MIT) in an ultrashort period $(LiOsO_3)_1/(LiNbO_3)_1$ superlattice. We used electronic structure calculations to predict that the $(LiOsO_3)_1/(LiNbO_3)_1$ superlattice exhibits strong coupling between magnetic and ferroelectric degrees of freedom with a ferrolectric polarization of 41.2 μC cm^{-2}, Curie temperature of 927 K, and Néel temperature of 379 K. The ferroelec-

Figure 13: (a) The $LiOsO_3/LiNbO_3$ superlattice exhibits the $a^-b^-b^-$ tilt pattern. Atom- and orbital-resolved DOS for (b) $LiOsO_3$, (c) $LiNbO_3$ and (d) $LiOsO_3/LiNbO_3$ at the DFT-LDA level.

tric properties mainly originate from cooperative Li and O displacements. We find that the insulating and magnetic state is driven by an enhancement of the electronic correlations in $LiOsO_3$ layers owing to the kinetic energy reduction of the t_{2g} orbitals from the superlattice geometry. **Our efforts have uncovered a promising alternative route to discovery of room-temperature multiferroics**: One could search for correlated *polar metals near Mott transitions* and drive the phases into insulating states, rather than the often-pursed approach of inducing polar displacements in robustly insulating magnets.
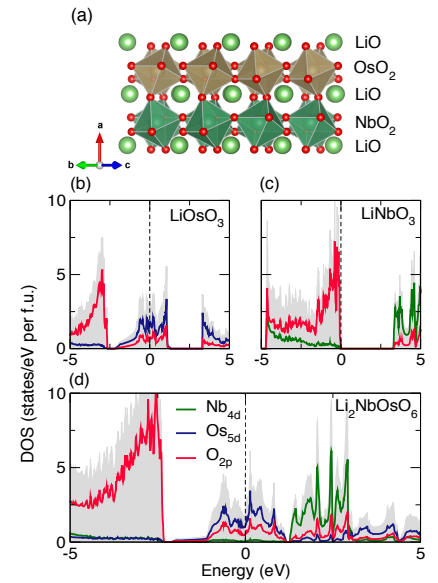
B.5. Correlation and Effects in Noncentrosymmetric Hund's Metals.

Using a first-principles approach based on density functional theory and dynamical mean field theory, we examined the electronic properties of a new candidate polar metal $SrEuMo_2O_6$ (SEMO). Its electronic struc-

ture shares similarities with centrosymmetric $SrMoO_3$ (SMO) and $EuMoO_3$ (EMO), from which it may be considered an ordered derivative, but ferroelectric-like distortions of the divalent cations and oxygen anions lift inversion symmetry mediated by an anharmonic lattice interaction in the metallic state. We find that Hund's coupling promotes the effects of electronic correlations owing to the Mo^{4+} d^2 electronic configuration, producing a correlated metallic phase far from the Mott state (Figure 14).

The ferroelectric-like state coexists with a correlated metallic phase which relies on the Hund's coupling and it is robust with respect to Mott localization. The contraindication between metallicity and polar distortions is thereby alleviated through the renormalized quasiparticles, which are unable to fully screen the ordered local dipoles, in the Hund's metal $SrEuMo_2O_6$.

Our main finding is that the poorly coherent quasiparticles are ineffective at completely screening the ordered local dipole moments. These results strengthen the link between correlated metallic states and the propensity of a metallic material to adopt polar structure, facilitating the selection or design of new correlated polar metals for enhanced magnetoelectronic responses or customized antisymmetric exchange interactions, which support exotic magnetic textures (helical or skyrmionic structures). This work was submitted for publication to *Physical Review Letters*, and can be found online as a preprint on the ArXiv.[33]

Figure 14: (Color online) Quasiparticle weights (Z) calculated within DFT+DMFT for SMO, EMO and SEMO at different values of the ratio J_H/U. Inset: Imaginary part of the inverse dielectric function, $1/\epsilon$, for SEMO at different J_H/U values.

Although our current understanding of polar metals reveals that most of them are in a correlated electronic regime with bad metallic behavior, we do not eliminate the possibility that non-correlated polar metals may exist; rather, **strong electronic correlations appears to be a favorable ingredient to stabilizing non-centrosymmetric metallic phases**, but it may not be a prerequisite in scenarios where the inversion lifting displacements are indeed decoupled from the low-energy electronic structure.

B.6. Polar Distortions in Vanadates.
Beyond the ruthenates and cuprates, we have actively been exploring the structure–property relationships in other transition metal oxides which are close the the metal-insulator phase boundary. In collaboration with the thin film growth group of Prof. Engel-Herbert (Department of Materials Science and Engineering, PennState), we investigated the strain effect on the electronic and magnetic properties of the correlated metal $SrVO_3$. The Engel-Herbert group was able to grow oxygen stoichiometric $SrVO_3$ under strain[34] which exhibits weak ferromagnetism. We note that in the literature the magnetic behavior of $SrVO_3$ is controversial. Generally $SrVO_3$ is described as a Pauli paramagnet.[35] However, Dougier et al. report a ferromagnetic spin density wave in bulk $SrVO_3$ with the appearance of a Pauli paramagnetic behavior on $SrVO_{3-\delta}$ for $\delta > 0.1$.[36]

In Figure 15 we show the calculated magnetic behavior of $SrVO_3$ as function of strain within Perdew-Burke-Ernzerhof revised for solids approximation (PBEsol)[37]. We found that the magnetic behavior of stoichiometric $SrVO_3$ can be tuned by subtle changes in the epitaxial strain, which we hypothesized is related to the Jahn-Teller tendency of the V^{4+} cation. The ferromagnetic phase becomes stable for small values of compressive and tensile strain consistent with the experimental observations. Because $SrVO_3$ is a strongly correlated metal, our results may be sensitive to correlations effects which we have not explicitly
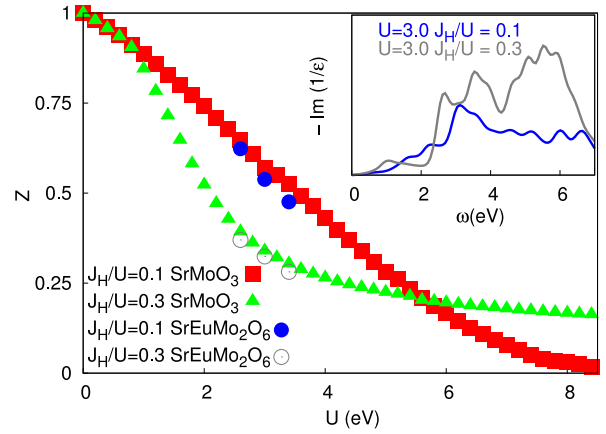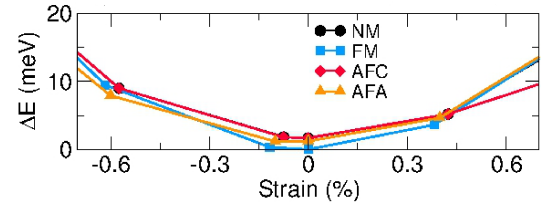

Figure 15: Energetic stability of various magnetic configurations of $SrVO_3$ as a function of strain calculated with PBEsol functional.

included. For this reason, we performed a series of calculations that include a small onsite Coulomb interactions (U=1 eV). We found essentially the same results for small values of strain. Moreover, we analyzed the possibility to induce rotations in $SrVO_3$ as function of strain and found that the rotations are disfavored in $SrVO_3$. Note that as part of this collaboration with the Engel-Hebert group, we have identified that *ultrathin film $SrVO_3$ may be an excellent transparent-conducting oxide.*

Finally, we examined 1/1 $SrVO_3$/$CaVO_3$ superlattices (with and without the additional Coulomb interactions) to guide our search for probable ground state atomic configurations. Our main results are that (1) neglecting the correlations produces a polar and metallic ground state crystal structure, and (2) when taking in account enhanced correlations, the crystal structure becomes centrosymmetric with space group $P\bar{1}$ and insulating ($U \geq 2$ eV). Such a correlation-induced metal-insulator transition makes the superlattice system, because it may be a candidate material for thermoelectric applications.

III.   Research Training and Development

The program supported researchers with multiple levels of expertise, including undergraduate (A. Cordi, who received a M.S. Degree) and graduate (J. Young) students and post-doctoral researchers (D. Puggioni and M. Gu). These researchers have become proficient or fluent in performing density functional theory calculations with the Vienna *Ab Initio* Simulation Package (VASP) and the AbInit package[38]. They have also learned how to use complimentary post-processing tools to understand lattice dynamical simulations and aid in the application of group theoretical studies to explain the behavior of noncentrosymmetric metals.

To provide professional development opportunities, all researchers supported by this award helped to prepare computational supercomputing hour proposals, from which the results described before were obtained. These efforts include the submission and preparation of grant proposals to the Center for Nanoscale Materials (CNM) at Argonne National Laboratory and the Extreme Science and Engineering Discovery Environment (XSEDE), which were subsequently awarded. These computational hours complement those made available from the DOD through the HPCMP. All researchers also presented work at the American Physical Society March Meetings in 2012-2015 and at other conferences. These experiences have improved each researcher's communication skills and have grown each persons professional network.

IV.   Research Dissemination

Publications   The award supported **14 journal article** publications. See the ARO Extranet Report for details.
Submitted Manuscripts

⋄ *Lifting Dirac nodes in topological semimetallic perovskite SrIrO3 through epitaxial constraint*, J. Liu, D. Kriegner, L. Horak, D. Puggioni, C. Rayan Serrao, R. Chen, D. Yi, C. Frontera, V. Holy, A. Vishwanath, J.M. Rondinelli, X. Marti, and R. Ramesh (Submitted, June 2015).

⋄ *Electronic correlations and screening effects in the Hund's polar metal $SrEuMo_2O_6$*, G. Giovannetti, D. Puggioni, J.M. Rondinelli, and M. Capone (Submitted, July 2015).

Manuscripts in Preparation

⋄ *Origin of the acentricity of the layered copper oxide superconductor $LaSr_2Cu_2GaO_7$*, D. Puggioni, and J.M. Rondinelli

⋄ *Stabilization of the polar phases in $LnSr_2Cu_2GaO_7$ (Ln=La, Y)*, D. Puggioni, and J.M. Rondinelli

⋄ *Polar Metals: Progress and Perspective*, Invited Topical Review for *J. Phys. Condens. Matter*, N.A. Benedek, and J.M. Rondinellit

Presentations   See electronic entries in the ARO Extranet Report.

VII.   References

[1]   J. Young and J. M. Rondinelli, Chemistry of Materials **25**, 4545 (2013).
[2]   J. Young and J. M. Rondinelli, Phys. Rev. B **89**, 174110 (2014).

[3]   G. Gou and J. M. Rondinelli, Advanced Materials Interfaces **1**, 1400042 (2014).

[4]   J. Young, A. Stroppa, S. Picozzi *et al.*, Dalton Transactions **44**, 10644 (2015).

[5]   P. W. Anderson and E. I. Blount, Physical Review Letters **14**, 217 (1965).

[6]   D. Puggioni and J. M. Rondinelli, Nature Communications **5**, 3432 (2014).

[7]   H. Wu, Z. Hu, D. I. Khomskii *et al.*, Phys. Rev. B **75**, 245118 (2007).

[8]   T. Maitra and R. Valentí, Physical Review Letters **99**, 126401 (2007).

[9]   A. T. Burkov, A. Heinrich and M. V. Vedernikov, AIP Conference Proceedings **316**, 76 (1994).

[10] A. B. Kaiser and C. Uher, in *Studies of High Temperature Superconductors*, Vol. 7, edited by A. V. Narlikar (Nova Science, New York, 1991) p. 353.

[11] W. P. S. Zeuner and H. Lengfellner, Applied Physics Letters **66**, 1833 (1995).

[12] M. P. Warusawithana, C. Cen, C. R. Sleasman *et al.*, Science **324**, 367 (2009).

[13] D. Puggioni and J. M. Rondinelli, Journal of Physics: Condensed Matter **26**, 265501 (2014).

[14] B. C. Webb, A. J. Sievers and T. Mihalisin, Phys. Rev. Lett. **57**, 1951 (1986).

[15] J. W. Allen and J. C. Mikkelsen, Phys. Rev. B **15**, 2952 (1977).

[16] H. Makino, I. H. Inoue, M. J. Rozenberg *et al.*, Phys. Rev. B **58**, 4384 (1998).

[17] D. G. Schlom, L.-Q. Chen, C.-B. Eom *et al.*, Annual Review of Materials Research **37**, 589 (2007).

[18] C.-J. Eklund, C. J. Fennie and K. M. Rabe, Physical Review B **79**, 220101 (2009).

[19] P. V. Ong and J. Lee, Journal of Applied Physics **112**, 014109 (2012).

[20] D. Puggioni and J. M. Rondinelli, Nat. Commun. **5**, 3432 (2013).

[21] K. Poeppelmeier, J. Thiel, J. Vaughey *et al.*, Physica C: Superconductivity **185-189, Part 1**, 525 (1991).

[22] J. T. Vaughey, J. P. Thiel, E. F. Hasty *et al.*, Chemistry of Materials **3**, 935 (1991).

[23] B. Hunter, J. Jorgensen, J. Wagner *et al.*, Physica C: Superconductivity **221**, 1 (1994).

[24] M. Isobe, Y. Matsui and E. Takayama-Muromachi, Physica C: Superconductivity **222**, 310 (1994).

[25] M. Fiebig, J. Phys. D: Appl. Phys. **38**, R123 (2005).

[26] W. Eerenstein, N. D. Mathur and J. F. Scott, Nature **442**, 759 (2006).

[27] R. Ramesh and N. A. Spaldin, Nature Materials **6**, 21 (2007).

[28] J. P. Velev, S. S. Jaswal and E. Y. Tsymbal, Philosophical Transactions of the Royal Society A: Mathematical, Physical and Engineering Sciences **369**, 3069 (2011).

[29] M. Bibes and A. Barthelemy, Nature Materials **7**, 425 (2008).

[30] D. Khomskii, Physics **2**, 20 (2009).

[31] H. Boysen and F. Altorfer, Acta Crystallogr. B **50**, 405Ð414 (1994).

[32] Y. Shi, Y. Guo, X. Wang *et al.*, Nature Materials **12**, 1024 (2013).

[33] G. Giovannetti, D. Puggioni, J. M. Rondinelli *et al.*, ArXiv e-prints (2015), arXiv:1507.00292 [cond-mat.str-el] .

[34] J. A. Moyer, C. Eaton and R. Engel-Herbert, Advanced Materials **25**, 3578 (2013).

[35] M. Rey, P. Dehaudt, J. Joubert *et al.*, Journal of Solid State Chemistry **86**, 101 (1990).

[36] P. Dougier, J. C. Fan and J. B. Goodenough, Journal of Solid State Chemistry **14**, 247 (1975).

[37] J. P. Perdew, A. Ruzsinszky, G. I. Csonka *et al.*, Physical Review Letters **100**, 136406 (2008).

[38] X. Gonze, J. Beuken, R. Caracas *et al.*, Computational Materials Science **25**, 478 (2002).